Unlimited

MICROMETEOROID STUDIES

STATUS REPORT - DECEMBER, 1966

FEB 1970
RECEIVED
NASA STI FA
INPUT BR

FACILITY FORM 602

N71-70623
(ACCESSION NUMBER)
(THRU)
39
(PAGES)
(CODE)
CR-116216
(NASA CR OR TMX OR AD NUMBER)
(CATEGORY)

JET PROPULSION LABORATORY
CALIFORNIA INSTITUTE OF TECHNOLOGY
PASADENA, CALIFORNIA

Sgt-64096R

DOCUMENT NO. VOY-C2-TM-10
December, 1966

MICROMETEOROID STUDIES

STATUS REPORT - DECEMBER, 1966

BY

R. C. Good
Space Sciences Laboratory

N. Behringer
MOL - Biosciences

F. Nayor
Advanced Interplanetary Programs

APPROVED BY R. P. Wolfson
R. P. Wolfson, Cognizant Eng.
Planetary Quarantine
Voyager Spacecraft System Proj.

PREPARED FOR

Jet Propulsion Laboratory
California Institute of Technology
4800 Oak Grove Drive
Pasadena, California

Under JPL Contract No. 951112

GENERAL ELECTRIC

Missile and Space Division
Valley Forge Space Technology Center
P. O. Box 8555, Philadelphia, Pa. 19101

STATUS REPORT

INTRODUCTION

The primary concern of the micrometeoroid studies reported herein is the possibility of contaminating Mars with unsterile particles ejected from the spacecraft surfaces as a result of micrometeoroid impacts. Two parallel activities -- an analytical and an experimental investigation -- are focused on defining this potential. This report is meant as interim documentation of the status of these activities through December, 1966.

Section I, Analytical Studies, details the work being performed by Dr. R. C. Good of the General Electric Space Sciences Laboratory. Early efforts in the analytical study were reported in Documents No. VOY-C2-TR-2 and VOY-C2-TM-4. The current effort, reported herein, is concentrated on the assembling and assimilation of published data in the form of quantitative relations for particles ejected by micrometeoroid impacts on the Voyager surface materials. The specific questions to which answers are being sought are as follows:

1) The total surface area affected,
2) The velocity of the ejected particles,
3) The mass distribution of the ejected particles.

Section II, Experimental Program, reports the work being performed by N. Behringer of the General Electric Biosciences Operation, MDL Department and by H. Semon of the General Electric Space Sciences Laboratory. This activity consists of subjecting typical spacecraft materials, seeded with microorganisms, to simulated micrometeoroid impacts. Much of the early experimental effort has been reported in detail in the General Electric Company, Voyager, Task C Bi-Monthly Progress Reports

Nos. 1,2, and 3. The test matrix for the current experimental effort was described in the Task C, Bi-Monthly Progress Report No. 4. Results of testing todate are reported herein.

SECTION I

ANALYTICAL STUDIES

SUMMARY

The work to-date on quantitative relations for particles ejected by meteoroid impacts on the Voyager surface materials is reported. Specific items are area of surface affected, the velocity of the ejected particles, and the mass distribution of ejected particles.

At this time we have assembled the published data in a form suitable for reporting as above. Several equations are given as derived from those data. In some cases error bands are indicated which represent the probable errors (0.6745 of the standard deviation). It is very possible that the equations will be corrected upon more detailed examination of the data. However, we are quoting them as an indication of the range. For convenience, some are given in this summary. Units are explained in the text at the quoted equations.

1. Flux to be met during the cruise portion of the flight:

$$N = 10^{-14.14 \pm 0.17} M^{-1.17 \pm 0.085} \qquad (1)$$

2. Flux to be met during the orbiting portion of the flight:

$$N = 10^{-15.58 \pm 1.28} M^{-1.37 \pm 0.23} \qquad (2)$$

3. Area affected in thick targets:

$$A = \pi H^{-2.37 \pm 0.23} p_o^{-4.11 \pm 0.69} 10^{-11.50 \pm 1.79} \qquad (12)$$

4. Area affected in thin targets:

Not resolved. Thin targets are those having a thickness less than 150% of p.

5. Velocity according to X-ray shadowgraphs:

$$U = (0.086 \pm 0.051) - (0.023 \pm 0.021) \frac{d}{d_o} \tag{13b}$$

See also Figure 3.

6. Velocity according to ballistic pendulum tests:

$$U = V \frac{1 - 0.263\, V^{0.365}}{\left(1.35 \times 10^{-3} V\right)^{-13.8}} \tag{17}$$

7. Mass Distribution according to X-ray shadowgraph:

$$\frac{m_d}{\Sigma m} = 10^{-1.33 \pm 0.75} \left(\frac{d}{d_o}\right)^{2.69 \pm 0.26}$$

I. INTRODUCTION

Planetary quarantine for the Voyager bus involves among many other items the loss of contaminated particles after impact by micrometeoroids. These particles may be ejected material produced by the splash after impact, they may be spalled material produced by shock waves from the impact, and/or they may be loose particles detached by the vibrations set up in the impacted surface structure by the impact. This report will treat the first type only.

Three subjects will be treated to the limit of our present investigation: (1) the total area of surface from which ejecta are produced per unit of time; (2) a velocity distribution of the ejecta; and (3) a size or mass distribution of ejecta.

In general, all quantities should include probable error bands so that a final probability may be derived. Some data can be developed to the point of error bands. Some relations have not been substantiated by experiment or by measurements so that they will be semi-educated estimates. Some relations will be proposed for use with different materials that may be highly conjectural but represent the present thinking to-date. And lastly, all relations must be used in velocity regions presently unattainable in controlled experiments so that extrapolation by factors of 2 to 8 is the order of the day. With these restrictions in mind, the following work will be presented.

II. SURFACE AREA DISTURBED BY IMPACTS

In order to obtain the surface area disturbed by impacts, the following steps will be required: (a) the flux of meteoroids which strike the surface must be assumed, measured, or specified; (b) the effects on the surface such as penetration, crater formation, and/or perforation must be interpolated from measurements on space vehicles or extrapolated from experimental data. The extent of surface area per crater must be included. Some historical background was presented in a previous report (Ref. 1). Meteoroid flux, crater formation, and ejected spray were discussed in general terms. Below, further data will be presented to provide a more quantitative basis for calculations.

A. Flux of Meteoroids

Measurements of meteoroid flux have been made by eye, camera, radar, sediment analysis, orbiting spacecraft instruments, and deep-space probes via telemetered signals. Data are presented as shown on Figure 1 where the flux of particles greater than a certain mass is plotted against that mass. It has been noted that the flux seems to be decreasing with time or with improved accuracy of measurement. These variations in data lead to error bands on the flux to be assumed. Of course, the paucity of data is an even greater factor in proposing fluxes in space away from Earth.

Nonetheless, to fix a basis for computations, the meteoroid environment has been fixed by the Jet Propulsion Laboratory (Ref. 2a) and will be quoted below.

Table I - Meteoroid Environment

Position	Particle Flux	Velocity Range Km/sec	Velocity Average Km/sec	Density gms/cm^3
Near Earth	log N= -17.0-1.70 log M	0-10 (rel. to Earth)	-	0.4
Cruise	log N= {from -13.80 -logM+log F; to -14.48 -1.34 log M + log F}	10-70	40	0.4
Stoney Particles	log N= -16.2 -0.77 log M+3.4(A-1)	10-70	40	3.5
Iron Particles	log N= -16.9 -0.76 log M+3.4(A-1)	10-70	40	7.7
Mars Flyby	log N= {from -13.40 - log M; to -14.08-1.34 log M}	10-70	40	0.4
Within one Mars radius	log N=-17.60 -1.70 log M	0-5 (rel. to Mars)	-	0.4
Stoney Particles	log N= -14.5 -0.77 log M			3.5
Iron Particles	log N= -15.2 -0.76 log M			7.7

Notes: N is the number of particles/m^{2}sec of mass M and greater.

F is a correction factor for the region between Earth and Mars.

Solar distance in Astronomical Units	F Value
1.0 - 1.25	1.0
1.25 - 1.36	3.0
1.36 - 1.43	5.0
1.43 - 1.49	3.0
1.49 - 1.56	2.5

A is one astronomical unit.

The regions of most importance for ejected particles striking Mars are late cruise and orbiting phases. Using the table above we find that for the cruise phase there is a maximum and a minimum flux. If we take this as covering 95% of the cases (which is an estimate), then the equation for the flux becomes:

$$N = 10^{-14.14 \pm 0.17} M^{-1.17 \pm 0.085} \qquad (1)$$

For the orbiting phase let us combine the fluxes outside and inside one Mars' radius equally and use cometary debris as 90% and the asteroidal particles as 10% (Ref. 2b). This leads to the following equation:

$$N = 10^{-15.58 \pm 1.28} M^{-1.37 \pm 0.23} \qquad (2)$$

B. Effects on the Surface

The impact process at hypervelocity conditions have been described in various ways. Generally, one starts at lower velocities

and works his way upwards. For example, Figure 2 shows velocity regions in which various results of the impact are found (Ref. 3). At low velocity, the projectile does not break up. At supersonic regions the projectile shatters. At hypersonic regions the projectile and target flow like liquids so that hydrodynamic equations are valid. Another description shows that at low velocities and in low strength targets the momentum of the projectile is important, whereas at high velocities and with highly resistive targets the energy content of the projectile is important (Ref. 4).

These two means of looking at the process indicate that extrapolations to higher velocities could either be governed by another process or by the energy relations. In this latter case we would use empirical relations corresponding to expressions for the projectile energy.

To determine the surface damage on the target, we will work through the following chain: Given a flux of meteroids we combine this with the penetration of the target to obtain crater size and hence surface area disturbed. The flux is given in Part II A.

1. Thick Targets

Crater size is a function of the penetration since the craters are very nearly hemispherical. The penetration in

semi-infinite targets has been fitted empirically by many but with the most success and general acceptance by two sets of authors: the Charters-Summers equation (Ref. 5) is

$$\frac{p}{d} = 2.25 \left(\frac{\rho V}{\delta c}\right)^{2/3} \tag{3}$$

and the Herrmann-Jones (Ref. 6a) is

$$\frac{p}{d} = 0.60\left(\frac{\rho}{\delta}\right)^{2/3} \log_e \left[1 + 25\left(\frac{\rho}{\delta}\right)^{2/3} \frac{\delta V^2}{H}\right] \tag{4}$$

or in a slightly less complicated form (Ref. 6b).

$$\frac{p}{d} = 0.36\left(\frac{\rho}{\delta}\right)^{2/3} \left(\frac{102\,\delta V^2}{H}\right)^{1/3} \tag{5}$$

in which

p = crater depth
d = representative dimension of the projectile such as its diameter.
ρ = projectile density in grams/cm^3
δ = target density in grams/cm^3
V = projectile velocity in Km/sec
c = sonic velocity in the target in Km/sec
H = Brinell hardness of target

We note that these equations have properties of the projectile and the target as factors and a constant used to adjust the scale. It is possible to be closer to the physical process involved if we follow Naumann (Ref. 7) and Heyda (Ref. 8) by adding the Hugoniot data to adjust the constant. This takes the form

$$\frac{p}{d} = \left[\frac{C + SU}{C^1 + S^1 (V-U)}\, \alpha\right]\left(102\ \frac{\rho V^2}{H}\right)^{1/3} \qquad (6)$$

where $C + SU = D$, the shock velocity in the target and $C' + S'(V-U) = D'$, the shock velocity in the projectile. u is the material velocity in the shocked portion of the target and C, S, C', S' are constants obtained from Hugoniot data (Ref. 9). The values of U are obtained by setting the pressure in the target equal to that in the projectile near the shockfront. The value of U for any velocity V is the solution to the equation

$$U^2\left[\rho S - \rho^1 S^1\right] + U\left[\rho C + 2\rho^1 S^1 V + \rho^1 C^1\right] = \rho^1 V (C^1 + S^1 V) \qquad (7)$$

where ρ is the density and the primed quantities refer to the projectile. Values for materials appropriate to spacecraft are given in Table II (Ref. 7).

Table II - Hugoniot Data

Material Surfaces	Density gr/cm	C Km/sec	S
Aluminum	2.70	5.37	1.339
Magnesium	1.73	4.493	1.266
Nylon	1.14	2.294	1.625
Fused Quartz	2.20	1.30	1.560
Meteoroidal Iron	7.85	3.800	1.580
Granite	2.66	2.75	1.406
Tuff	1.70	1.50	1.400
Porous Aluminum	.44	.035	1.281

The penetration then is proportional to the cube root of the projectile energy. In eq. (6), and the 1st factor is asymptotic to a constant as the velocity increases. For a porous aluminum projectile (which is similar in density to a micrometeoroid) impacting an aluminum target the first factor in eq. (6) approaches .36 x .450 or .162 as indicated by Table III.

Table III

Impact Velocity Km/sec	$\frac{C+SU}{C'+S'(V-U)}$	$\frac{C+SU}{C'+S'(V-U)} \times .36$
10	0.739	0.266
20	0.568	0.204
30	0.514	0.185
40	0.488	0.176
50	0.473	0.170
60	0.462	0.166
70	0.455	0.164
80	0.450	0.162

If we choose other targets found on Voyager and other materials found in meteorites this factor will have other values.

Since Dalton (Ref. 6b) has given a tolerance on the penetration formula, the above data can be like amended to

$$\frac{p}{d} = (0.19 \pm 0.04) \left(\frac{102 \rho v^2}{H}\right)^{1/3} \tag{8}$$

To obtain the crater size we assume a hemispherical cavity with a radius of p. There will be a distribution of crater sizes because the factor d has a distribution given by Equation 2. Assuming spherical particles, the mass is given by

$$m = \frac{\pi}{6} \rho d^3 \tag{9}$$

so that the penetration is now given by

$$p = 10^{0.654 \pm 0.162} \left(\frac{m}{H}\right)^{1/3} \tag{10}$$

where the distribution of velocities of the meteoroids has been assumed to be Gaussian between 10 and 70 Km/sec and an average of 40 Km/sec. The angular distribution of impact was assumed uniform over 2 π steradians.

By differentiating Equation 2 and using Equation 10, we find that the number of craters of depth p per m^2sec is

$$\phi = 10^{-15.44 \pm 1.28} H^{-2.37 \pm 0.23} p^{-7.11 \pm .69} \tag{11}$$

Therefore, the total area of original surface deleted per square meter per second is given by

$$A = \pi H^{-2.37 \pm 0.23} \, 10^{-11.50 \pm 1.79} \, p_o^{-4.11 \pm 0.69} \qquad (12)$$

where p_o is minimum recognizable penetration.

2. Thin Targets

For targets which are perforated the portion of surface affected is smaller. In this case we have data taken by Gehring (Ref. 10) at velocities up to 16.5 Km/sec. The empirical equation is

$$\frac{D_s}{d} = 0.45 \, V \left(\frac{t_s}{d}\right)^{2/3} + 0.90 \qquad (13a)$$

where D_s is the diameter of the perforation, d is the diameter of the projectile, t_s is the target thickness, and V is the projectile velocity in Km/sec. In that paper no data are given on ejected particles so that many parts of the surface will be splashed towards the rear face and beyond. Even less has been studied on material ejected in this case than in the thick target case.

It would be difficult to compare Equation 7 and 13 because a thickness factor occurs in 13 and a hardness factor in 7 as well as the difference in the exponent of the velocity. Any statements on Equation 13 would be highly conjectural so that we could omit such effects. Further effort is dependent on the results of the experimental activities currently in progress.

III. VELOCITY DISTRIBUTION OF EJECTA

A. Direction

As a high speed particle impacts a solid and does not perforate it, a splash of ejecta is thrown back made up of many particles. When the projectile impacts the surface perpendicularly, the ejecta is symmetrically arrayed about the impact point. When the projectile impacts the surface obliquely, the ejecta spray pattern is biased in a direction along the projectile flight direction, as one would expect. For a spacecraft in space the meteoroid flux has randomly distributed velocity vectors (Ref. 26) so that one would expect impact on all sides from all directions because its velocity is an order of magnitude less than that of the meteoroids. For those reasons we can assume that the direction of ejecta leaving the Voyager will also be randomly distributed uniformly over all 4π steradians. This means that only the speed is amenable to calculation.

B. Magnitude

Measurements of the velocity magnitude have been made using momentum traps (Ref. 11, e. g.), heating effects (Ref. 12, e.g.), photographically (Ref. 13, e. g.), and aerodynamically (Ref. 14, e.g.). These show varying results as explained previously in Ref. 1. We may say that the tests use averaging methods since the individual particles have not been followed. Actually, time lapse photography should be most fruitful and some day this may be done successfully.

We may note that usually the mass and velocity are measured together as momentum or energy so that they are not singly available. Furthermore, measurements are not made on single impacts but over several which are not necessarily repeatable in all respects. With this in mind, we will show some results taken as averages.

In Ref. 1, average velocities for spray particles as a whole were calculated from X-ray shadowgraphs. Further work indicates that similar calculations may be broken down into various sizes of particles. When this is done one obtains a velocity vs. particles mass relation. Figure 3 shows the results with error bands indicated. The equation for the velocity in Km/sec is

$$U = (0.086 \pm 0.051) - (0.023 \pm 0.021) \frac{d}{d_o} \qquad (13b)$$

where d_o is the average particle diameter 43.3 mils and d is the diameter of the particles in mils. We note the large probable errors. We also note the low velocities in comparison with the impact velocity (5 Km/sec for these tests). Ref. 1 shows that the velocity of the ejecta should be roughly 45% of the projectile velocity on gross theoretical calculations.

Ref. 15 shows data on spray particle velocity taken by measuring the passage of burning ejecta with photomultipliers. With impacts at

2 Km/sec of stainless steel balls 3/16" diameter onto carbon steel targets, the spray velocity was clocked at 5-10 Km/sec. Because these are old data, they are difficult to reconcile, and no data since have repeated such high measurements, we have no choice but to note these conflicting data and go on.

Ref. 11 reports data on a momentum trap experiment in which pellets of polyethylene at velocities up to 7.8 Km/sec impacted an aluminum target. The data are fairly linear so that some inferences may be drawn. One graph shows the pendulum momentum vs. the projectile momentum. A rough fit shows

$$M_{pend} = 0.263 (M_{proj})^{1.365} \tag{14}$$

where M stands for momentum in ft. lbs./sec. Another figure shows the change in pendulum mass (which would be the ejecta mass) vs. the impact velocity. A rough fit shows

$$\frac{\Delta m_{pend}}{m_{proj}} = -13.8 + \left(1.35 \times 10^{-3}\right) V \tag{15}$$

where V is the projectile velocity in ft/sec. Let us write the momentum conservation relation as

$$M_{proj} = M_{pend} + M_{ejecta} \tag{16}$$

so that by combining 14-15-16 we obtain the velocity of the ejecta as

$$U = \frac{V - 0.263\, V^{1.365}}{-13.8 + \left(1.35 \times 10^{-3} V\right)} \tag{17}$$

We note that if V is 40 km/sec (the average meteoroid velocity) that U is 0.61 Km/sec which is much smaller (1.5%) than the impact velocity. At least these experiments have some tests at velocities approaching meteoroid velocities.

IV. MASS DISTRIBUTION OF EJECTA

As noted in the last section, most measurements combined the mass and velocity into the momentum or energy. Therefore, it is difficult to find measurements taken separately. There are three which can be presented.

Using the data of Kineke's X-ray shadowgraphs (Ref. 13), we have obtained a mass distribution relation. From the size, position, time data, the proportion of particles of a size d is the equation

$$\frac{m_d}{\Sigma m} = 10^{-1.33 \pm 0.75} \left(\frac{d}{d_o}\right)^{2.69 \pm 0.26} \qquad (18)$$

where m_d is the mass of all particles of the same size and therefore the same diameter, s

Σm is the total mass of the ejecta measured on the shadowgraph, and

d_o is the average size particle as in Section III. This should be coupled with the total mass ejected as per Denardo's data given in Equation 15 which in turn should be coupled with the flux Equation given in Section II.

A second method for obtaining a mass distribution was given by Cannon (Ref. 14) as a set of equations. Here the size of the particle is determined by its rate of burning in air; that is, viscous forces cause heating, burning, and demise of the particle. Thus, by

measuring the range, assuming the viscosity, and measuring the brightness photographically to obtain the burning rate, one can work back to the particle diameter. These calculations were not completed but could be by others.

A second method was introduced (Ref. 14) by the same laboratory in which the spray particles were allowed to strike an aluminum target and later count the craters so formed. They attributed the crater diameter to the particle diameter and assumed that their velocity was constant. By their own admission just above, the velocity will vary with particle range because of viscous forces. However, their data show 58% less than 5 microns, 99.5% less than 25 microns, and 0.5% greater than 25 microns.

REFERENCES

1. Good, R. C., "Preliminary Assessment of the Micrometeoroid Phenomena for the Planetary Quarantine Study - Voyager Task C", Doc. No. VOY-C2-TR2, July 1966, General Electric Company.

2a. Hess, D. S. and E. Pounder, "Voyager Environmental Predictions Document", Jet Propulsion Laboratory, SE 003 BB001-1B28, File SE1DB-6J-003, October 26, 1966.

2b. Volkoff, J. J., "Protection Requirement for the Resistance of Meteoroid Penetration Damage of Interplanetary Spacecraft Systems", JPL Tech. Report No. 32-410, July 1964.

3. Kruszewski, E. T., "Meteoroids: Needs for Penetration Sealing Laws and the Potentials of Simulation Techniques", Proc. of Conf. on the Role of Simulation in Space Technology, August 1964, No. 4, P&A, pg. IV-28, Va. Poly. Inst.

4. Rinehart, J. S., "Meteor Distribution and Cratering", Proc. 2nd Hypervelocity Impact Effects Symposium, pp. 45-53.

5. Summers, J. L. and A. C. Charters, "High Speed Impact of Metal Propestiles in Targets of Various Materials", Proc. 3rd Hypervelocity Impact Symposium, October 1958, Chicago, Ill.

6a. Herrmann, W. and A. H. Jones, "Survey of Hypervelocity Impact Information Addendum", ASRL Report 99-1, M.I.T., Cambridge, Mass., October 1961.

6b. Dalton, C. C., "Estimation of Tolerance Limit for Meteoroid Hazard to Space Vehicles 100-500 Kilometers above the Surface of the Earth", NASA TND-1996, Feb., 1964, pg. 44.

7. Naumann, R. J., "A Physical Basis for Scaling Hypervelocity Impacts", Proc. 7th Hypervelocity Impact Symposium, Vol. IV, pg. 1, February 1965.

8. Heyda, J. F., Personal communication, Space Sciences Laboratory, General Electric Co., King of Prussia, Pa.

9. Rae, W. J., "Final Report on A Study of Meteoroid Impact Phenomena, CAL, Report No. RM-1655-M-4, February 1963.

10. Göring, J. W. and A. B. Wenzel, "Hypervelocity Impact Studies against Apollo-Type Structures up to 16.5 Km/sec", GM Def. Research Laboratory, TR 65-56, July 1965.

11. Denardo, B. P., "Measurements of Momentum Transfer from Plastic Projectiles to Massive Aluminum Targets at Speeds up to 25,500 ft/sec", NASA TND-1210, March 1962.

12. Turner, G. H. and E. P. Palmer, "Energy Partitioning in High-Velocity-Impact Cratering in Lead", BSD-TDR-64-95 Part I, May 1964, Utah Research and Development Co., Salt Lake City, Utah.

13. Kineke, J. H., Jr., "Observations on Crater Formation in Ductile materials", 5th Hypervelocity Impact Symposium, Vol. I, Part 2, Page 339, October 1961.

14. Cannon, E. T., "Terminal Ballistic Investigation of the Impact and Effect of Ultra-High Speed Micron-Size Particles Produced on Hypervelocity Impact", APGC-TDR-62-69, Nov., 1962, ASTIA Doc. No. 291822.

15. Clark, W. H., R. R. Kadesch, R. W. Grow, "Hypervelocity Impact Spray Particles", AFOSR No. TN-60-990, May 1, 1960.

16. Gault, D. E., E. M. Shoemaker, and H. J. Moore, Spray Ejected from the Lunar Surface by Meteoroid Impact, Ames Research Center, NASA TND-1767, April 1963.

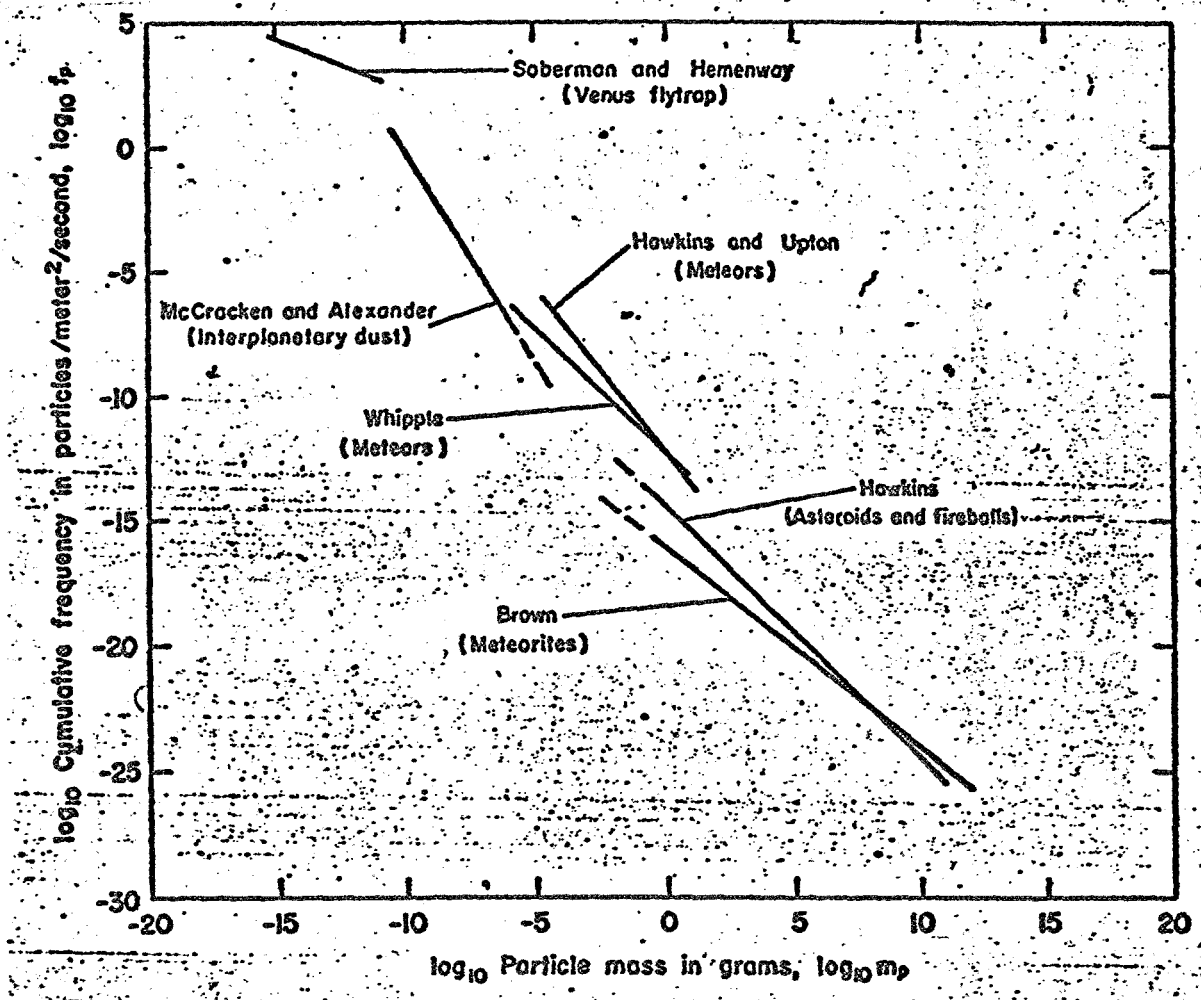

Figure 1.- Cumulative frequency-mass distributions for interplanetary debris.

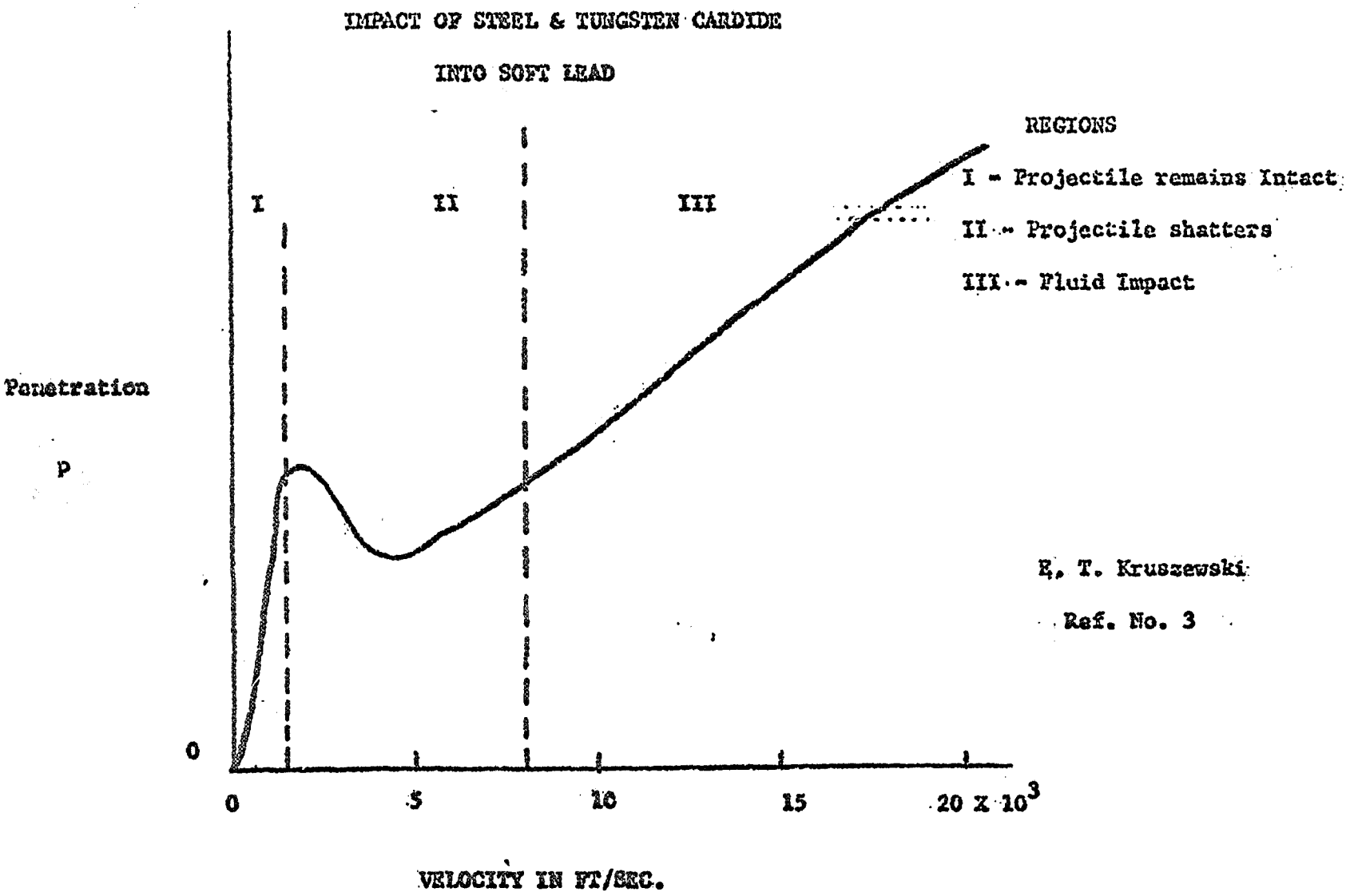
IMPACT OF STEEL & TUNGSTEN CARBIDE
INTO SOFT LEAD
REGIONS
I - Projectile remains Intact
II - Projectile shatters
III - Fluid Impact
I
II
III
Penetration
P
0
0
5
10
15
20 X 10^3
VELOCITY IN FT/SEC.
E. T. Kruszewski
Ref. No. 3

FIGURE 2

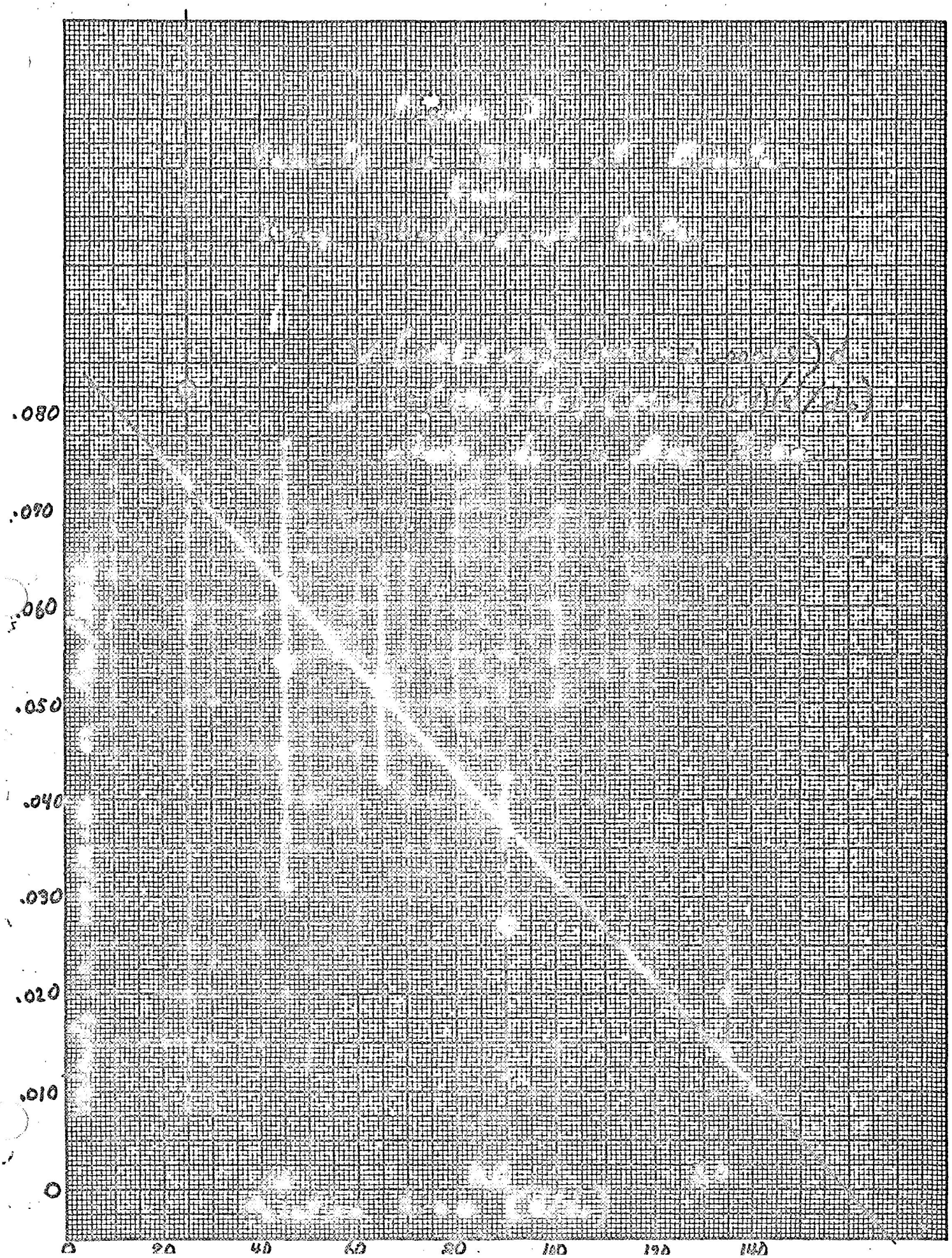
.080
.070
.060
.050
.040
.030
.020
.010
0
0
20
40
60
80
100
120
140

SECTION II

EXPERIMENTAL PROGRAM

GENERAL ELECTRIC
MISSILE AND SPACE DIVISION
PHILADELPHIA

PROGRAM INFORMATION [redacted]/RELEASE

*CLASS. LTR.	OPERATION	PROGRAM	SEQUENCE NO.	REV. LTR.
PIR NO. 7420-66-205(V30)				

*USE "C" FOR CLASSIFIED AND "U" FOR UNCLASSIFIED

FROM: F. S. Mayor/N. W. Behringer
Room M7034
Valley Forge

TO: R. P. Wolfson, Voyager Project
Pasadena Office

DATE SENT	DATE INFO. REQUIRED	PROJECT AND REQ. NO.	REFERENCE DIR. NO.
12/30/66			

SUBJECT

STATUS REPORT - EFFECTS OF SIMULATED MICROMETEOROID IMPACT TESTS ON MICROBIOLOGICALLY CONTAMINATED SURFACES

INFORMATION [redacted]/RELEASED

The objective of this experimental program is to determine the number of viable organisms released from a seeded (artificially contaminated) target due to the impact of hypervelocity particles. The feasibility and developmental efforts of this program have been successfully completed and the formal test series has recently been initiated. Four spacecraft materials, representing those surfaces which will be predominantly exposed to micrometeoroid impacts, are to be used as targets. Testing to date has included only aluminum targets; being seeded at both 10^3 and 10^8 spores per target (an area 0.02 in.^{2} was contaminated). Preliminary results indicate that anywhere from 0.5% to 15% of the inoculated spores may be released in a viable state due to impact depending upon such factors as target material and number of hits.

DISCUSSION

A. Background

As a result of the fabrication, shipping, handling and launch operations associated with interplanetary spacecraft, some degree of viable contamination will be present on all spacecraft (not required to be sterilized) surfaces. As a part of the current Voyager Planetary Quarantine studies, the program reported herein was initiated to quantitatively determine the level of this viable surface contamination which could be released by the impaction of micrometeoroids during space flight.

The initial experimental effort in this program consisted of a test series to evaluate the feasibility of collecting organisms that have been ejected due to hypervelocity impacts. The series evaluated several collection devices, target inoculation techniques and collection media. These feasibility test activities and the associated development of biological techniques and procedures has been thoroughly described in the Voyager, Task C, Bi-Monthly Progress Reports Numbers 1, 2, and 3.

The feasibility effort produced significant success. Viable ejecta could be collected and the amount collected varied directly with the level of seeding employed. The test apparatus, after several modifications is as shown in Figure 1. All testing is conducted at the General Electric Company Hypervelocity Test Facility in Morgantown, Pennsylvania.

PAGE NO.	RETENTION REQUIREMENTS: COPIES FOR	MASTERS FOR
OF	1 MO.	3 MOS.
	3 MOS.	6 MOS.
	6 MOS.	12 MOS.
	MOS.	MOS.
		DO NOT DESTROY

B. Test Materials

Voyager-type interplanetary spacecraft are composed of many materials, both metallic and non-metallic. A survey was conducted to determine which of the various materials would constitute a significant surface area of the prospected spacecraft and would therefore be more apt to be subject to micrometeoroid impact.

Document No. VOY-C2-TM4 reports the results of this survey, detailing all the pertinent spacecraft materials. For the purposes of this test program, only those materials with exposed surface areas greater than 50 ft.^{2} were considered critical. The materials chosen for testing were:

- 6061 Aluminum (40 mils thick)
- 2024 Aluminum (3 mils thick
- Textolite (15 mils thick)
- Fused Silica (15 mils thick)

The aluminum target materials were coated a thermal control paint on one side (the surface to be bombarded). All target materials have been acquired for testing.

C. Laboratory Procedures

All microbiological procedures, including target and apparatus sterilization, inoculant preparation and seeding, and post-test assays are conducted at the General Electric Bioscienses Laboratory in Valley Forge, Pennsylvania.

The target materials are "bio-cleaned"[1] and sterilized prior to seeding. Seeding is accomplished by depositing approximately 0.01 milliliters of a Bacillus subtilis var. niger spore suspension onto the center of the target. This droplet dries to form a contaminated area of approximately 0.02 in.^{2}. The spore suspension may be diluted, as required, to achieve the desired contamination level. After seeding, the contaminated targets are stored in sterile petri dishes until ready for insertion into the test apparatus. A seeded target is shown in Figure 2.

The apparatus is sterilized in Ethylene oxide-freon mixture (12% Ethylene oxide; 88% Freon-12) prior to each test. External sterility of the apparatus is lost during transport to the test site, but sterility of the internal surfaces is maintained.

The micrometeoroid trap, shown schematically in Figure 3, is designed to collect both front (top) and back (bottom) face ejecta from the targets. The targets are seeded on both sides. The trap is sterilized with Ethylene oxide-Freon mixture prior to the addition of the gelatin collection medium

[1] According to the techniques for cleaning stainless steel strips in NASA Standard Microbiological Examination of Spacecraft Hardware

Previously the gelatin was liquified and then passed through through 0.45 micron filter. The filter, then containing the ejected micro-organisms, was blended and plated with Trypticase Soy Agar[1] for subsequent incubation.

The gelatin, due to the large number of organisms being collected, is now assayed directly. A sample of gelatin is removed and diluted for the assay. This has eliminated the time consuming filtration portion of the technique previously used. The gelatin sample is sonicated to break up any "clumping" of organisms. Trypticase Soy Agar is the plate count medium. The plates are then incubated in an inverted position for 72 hours at 37°C and are observed, colonies produced being counted at intervals of 24, 48 and 72 hours. The results listed in Figure #5 were obtained by using the above exposure and assay technique.

D. Test Program

The formal test series will consist of 32 required tests and several intermediate test points. The required tests consist of the following:

MATERIAL	INOCULATION LEVEL HIGH (10^8)	INOCULATION LEVEL LOW (10^2 - 10^3)
Aluminum 6061	X X X X	X X X X
Aluminum 2024	X X X X	X X X X
Textolite	X X X X	X X X X
Fused Silica	X X X X	X X X X

The eight test points, plus some intermediate data points for each material should provide a statistically valid data sample for meaningful interpretation.

Several tests will be conducted at inoculation levels between 10^3 and 10^8 to establish the shape of any developed relationship between the levels bombarded and the quantity of ejecta recovered. These intermediate points will be conducted as time and schedule permits.

As shown in Figure 4, the post-test condition of a target indicates impaction by many particles. Current data analysis effort is attempting to establish a correlation between the viable organisms collected and the actual total area of impaction. Hits and hit sizes are being determined microscopically for this analysis.

[1] Trade name of Baltimore Biological Laboratories, Baltimore, Md.

E. Results

At this point in time, about 50% of the required tests have been completed. Figure 5 presents a compilation of the data collected to date. It should be noted that the data presented are direct assay results and have not been correlated with impaction areas. Also, the data is reported for the assays of the ejecta from the top target surfaces only.

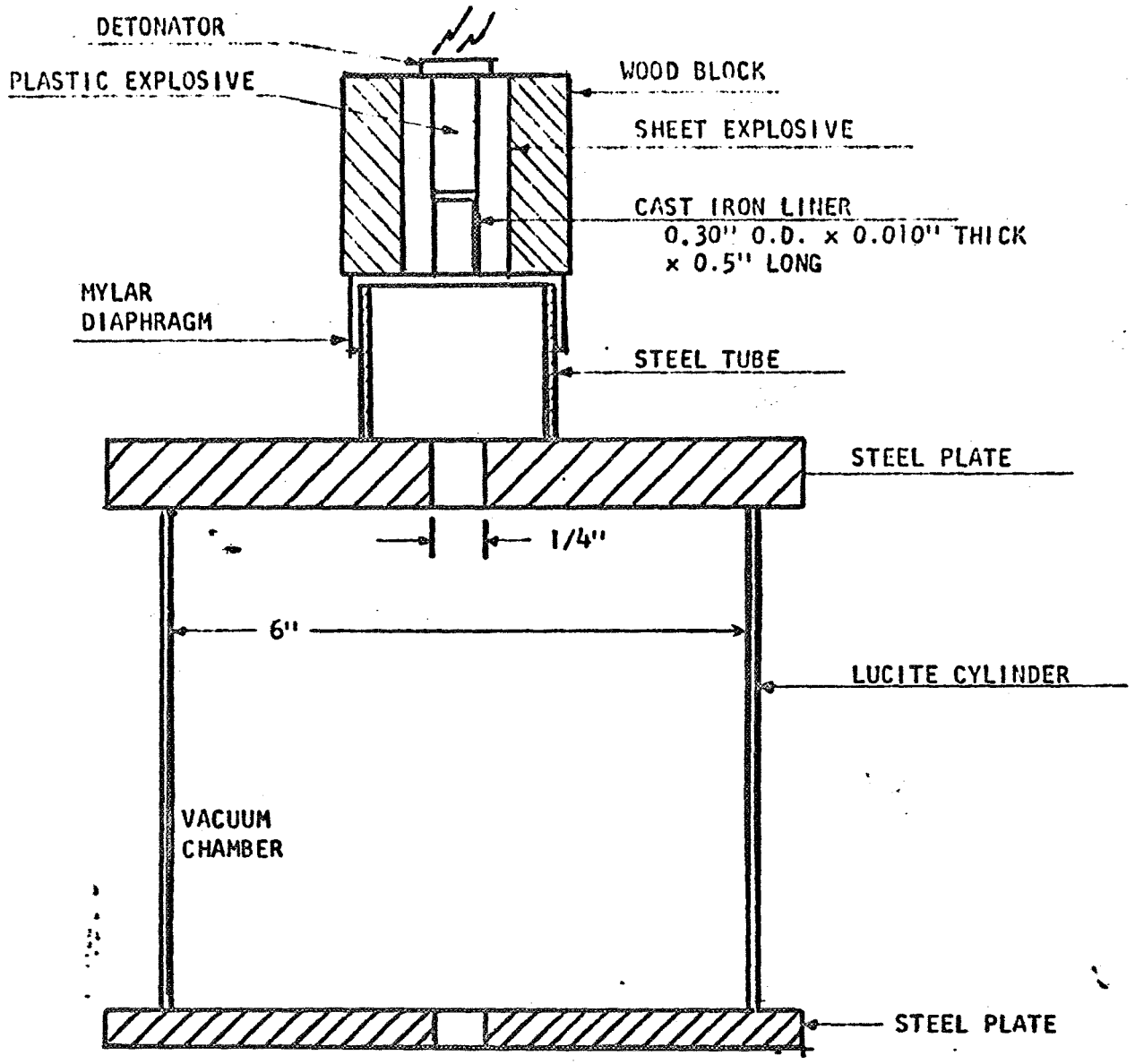

MICROPARTICLE PROJECTOR

Figure 1

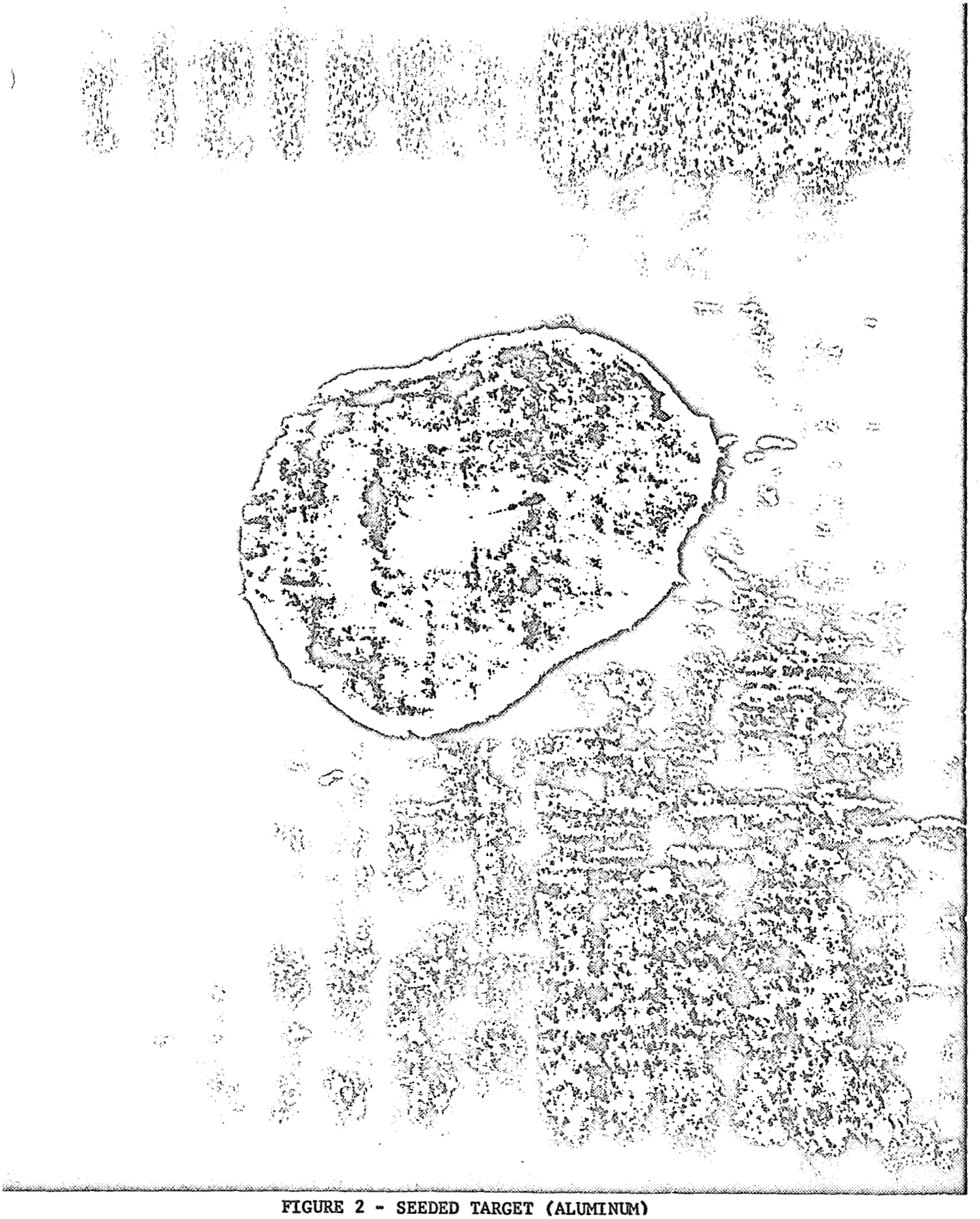

FIGURE 2 - SEEDED TARGET (ALUMINUM)

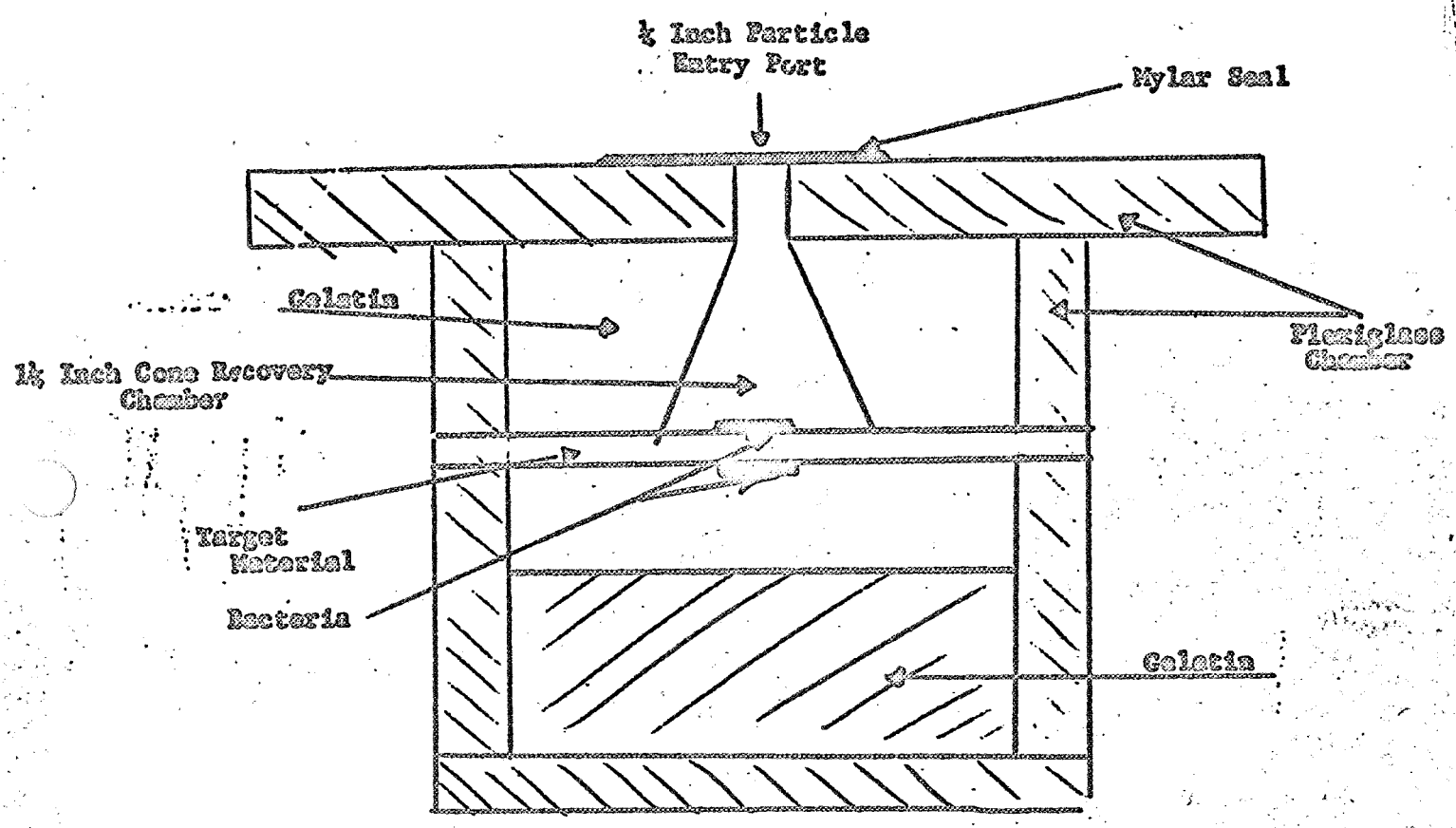

MICROMETEOROID TRAP
- SCHEMATIC -

Figure 3

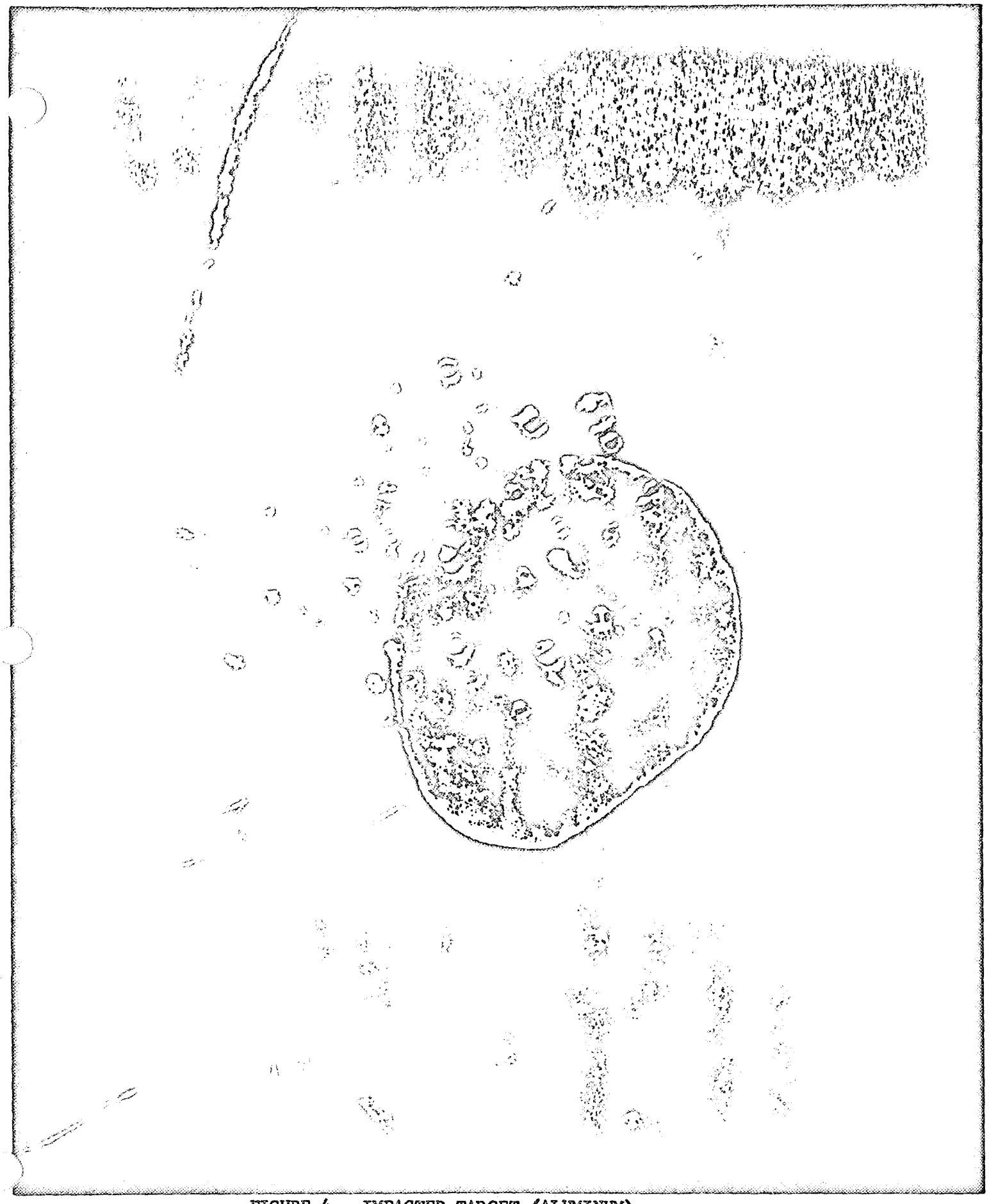

FIGURE 4 - IMPACTED TARGET (ALUMINUM)

FIGURE 5 - SUMMARY OF LEVELS OF ORGANISMS RECOVERED FROM TRAPPED EJECTA PRODUCED BY SIMULATED MICROMETEOROID IMPACT ON ACTUAL SPACECRAFT MATERIALS

INOCULATION LEVEL	MATERIALS			
	6061 ALUMINUM (40 mils)[1]	2024 ALUMINUM (3 mils)	TEKTOLITE (15 mils)	FUSED SILICA (15 mils)
High Level ($\sim 10^8$)	1.65×10^8 3.73×10^6	1.06×10^8 2.18×10^7		
	1.65×10^8 1.73×10^6	1.06×10^8 2.48×10^7		
	1.65×10^8 3.67×10^6	1.06×10^8 7.23×10^6		
	1.65×10^8 1.51×10^5	1.06×10^8 9.73×10^6		
Low Level ($10^2 - 10^3$)	6.2×10^2			
	6.2×10^2			
	6.2×10^2			
	6.2×10^2			
Intermediate Levels (conducted as time permits)	1.8×10^7 9.92×10^4			
	1.8×10^6 7.4×10^5			
	1.8×10^5 2.1×10^4			
	1.8×10^4 7.5×10^2			

KEY:*

(1) Inoc. Level/Post-Test Assay; shaded areas yet to be completed.
(2) All targets contaminated on both sides
(3) Assays reported for top surface only
(4) Assays <u>not</u> related to hit area
(5) Top side of Aluminum targets coated with thermal control paint.